Memo on Completion of Task 2 of Pooled-Fund Skewed Abutment Testing with Rotation and Translation Study

Date: Sept. 1, 2025
To: David Stevens, Project Manager, Research Group, Utah Dept. of Transportation
From: Kyle Rollins, PI, Civil and Construction Engineering Dept., Brigham Young Univ.

We have completed the work associated with Task 2-Performance of large-scale skewed abutment tests. Lateral load tests were performed on the simulated abutment with skew angles of 0°, 15°, 30°, and 45° relative to the direction of loading. The backfill consisted of washed concrete sand compacted to 95% of the modified Proctor maximum density as in previous tests; however, the maximum Proctor density was 116.5 pcf in comparison to 111.5 pcf in the previous series of tests performed with longitudinal loading. The passive force provided by the backfill was determined by loading the abutment before and after compacting backfill behind the abutment. As with previous tests, we measured the applied lateral force, abutment displacement and rotation, pressure on the backwall, vertical and horizontal movement of the backfill, and the location of the failure surface in the backfill. However, in contrast to previous tests, the load was applied with an actuator on the opposite side from the acute corner and the abutment was allowed to rotate as it was pushed longitudinally. This led to significant rotations, that increased as the load increased.The difference in movement from one side of the abutment to the other reached 1 to 1.5 inches.

Fig. 1 shows the measured passive force vs. abutment deflection plots for the four passive force tests. For the 0° and 15° skew tests the passive force curves are very similar with little reduction in resistance with skew. In contrast, the passive force decreases substantially as the skew angle increases to 30° and then 45°. The peak passive force for rotation and longitudinal displacement was typically 55 to 75% of that measured previously for longitudinal displacement only. The peak passive force for each test occurred between 3% and 4% of the wall height in each case. However, in contrast to previous longitudinal tests, the passive resistance typically decreased substantially after reaching the peak force down to some low residual value. The passive resistance for the 45° test is likely somewhat lower than it should be because compaction control used the 111.5 pcf maximum Proctor density instead of the 116.5 pcf value that was later obtained for the new fill material, a difference of 4.5%.

The reduction in the post-peak passive force, when the abutment rotates and produces a non-uniform pressure on the backfill, is consistent with 3-D finite element computer analyses of passive force on skewed abutments reported by Shamsabadi et al. (2006) for

rotational loading as shown in Fig. 2. The rotational movement is assumed to produce a triangular pressure distribution on the back face of the bridge abutment.

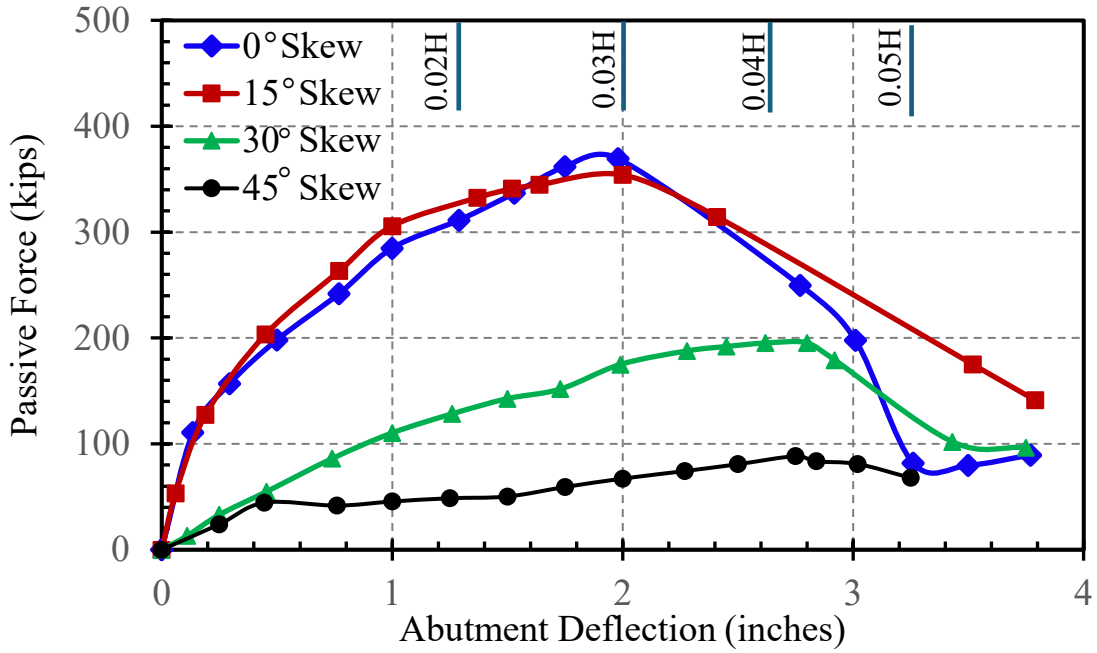

Fig. 1. Passive force vs. Abutment deflection curves for each of the four passive load tests with translation and rotation.

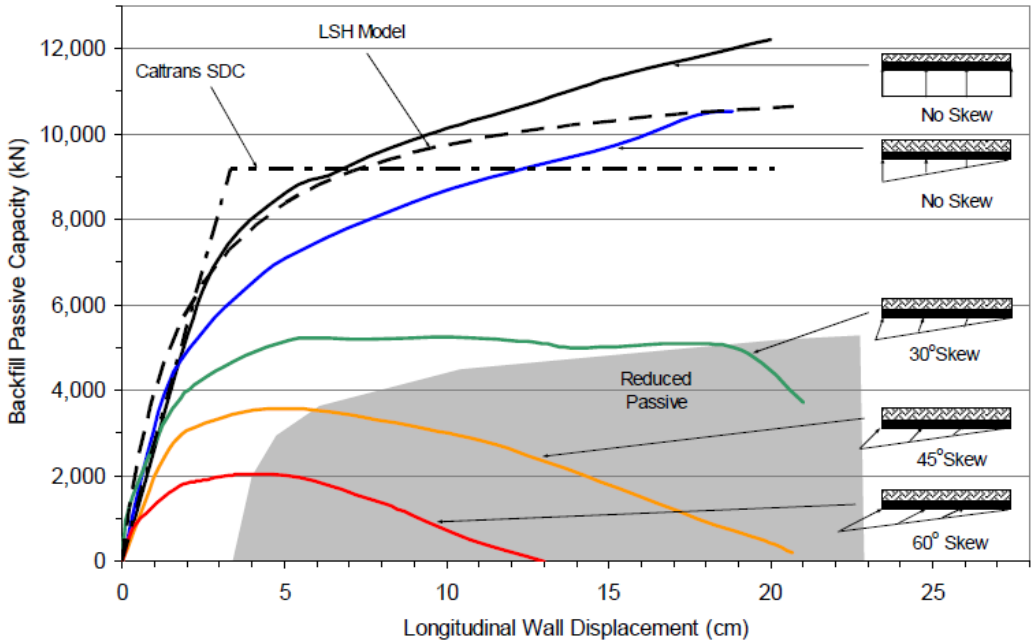

Fig. 2 Effect of bridge skew angle on passive force-deflection curves based on 3D finite element analyses reported by Shamsabadi et al. (2006).

During each passive force test, the heave of the backfill was measured over a uniform grid using an autolevel with an accuracy of 0.001 ft (0.01 inch). For the 30° and 45° skew tests, heave was significant within about 6 feet behind the abutment wall, but decreased significantly beyond this distance. For each test, two longitudinal trenches were excavated in front of the abutment wall to identify the shear planes. For the non-skewed test (Θ = 0°), the typical log spiral shear plane was clearly identified in each trench as shown in Fig. 3. In addition, a 3D failure surface daylighted within the backfill zone as shown in Fig. 4. In contrast, for the skewed tests, the shear planes could only be identified up to a distance of about 5 feet from the wall but then disappeared at greater distances. In addition, no clear failure surface daylighted in the backfill although heave was present.

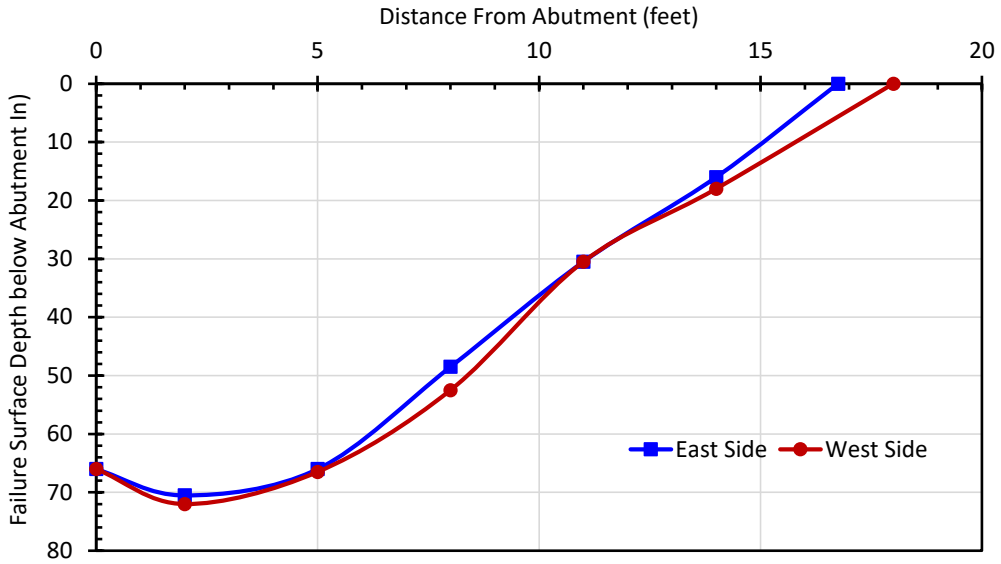

Fig. 3 Depth of failure surface vs. distance from the abutment wall for the no skew (Θ = 0°) test showing typical log-spiral failure geometry.

In the FEM studies of skewed abutments during rotation, Shamsabadi et al. (2006) report that "the mobilized passive capacity might decrease at large displacement levels (see shaded area in Fig. 2). At very high-skew abutments, the passive capacity can decrease to zero, which is a result of "disintegration" of the passive wedge after significant plastic ground deformation and heave has occurred." This "disintegration" of the passive failure wedge, accompanied by decreased passive resistance, appears to be what was observed in these field tests where the shear planes disappeared. Additional validation of computer models with the measured results along with additional numerical modeling of different geometries will be necessary in Task 5 to understand better the mechanisms involved in this phenomenon.

Fig. 4 Photograph of backfill with red grid for no skew (Θ = 0°) test along with failure surface daylighting (green spray paint) with three-dimensional geometry.

One of the important goals of this study was to determine if the passive force reduction factor (R_{skew} or R_{Θ}) would be different than that developed based on longitudinal loading only. Based on the results from the passive force tests with both longitudinal deformation and rotation, the measured R_{skew} factors are 1.0, 0.96, 0.53, and 0.24 for the 0°, 15°, 30°, and 45° skew tests, respectively. These R_{skew} factors are plotted vs. skew angle in Fig. 5 along with the results from previous longitudinal passive force tests (Rollins and Jessee 2013, Rollins et al. 2019) and numerical analyses reported by Shamsabadi et al. (2006). A Best-fit design curve proposed by Shamsabadi and Rollins (2014) is also provided for comparison purposes. The R_{skew} for the 15° test is clearly an outliner relative to the rest of the data points and it is unclear if this is a simply a result of the rotation or some other factor. The R_{skew} for the 30° test is very close to the design curve while R_{skew} for the 45° test is just below the bottom of the scatter for all the test data. Part of the discrepancy for the 45° test may result from the somewhat lower compaction of the backfill which likely led to less passive resistance. Additional numerical analyses will be necessary to provide additional insight regarding the interpretation of these test results.

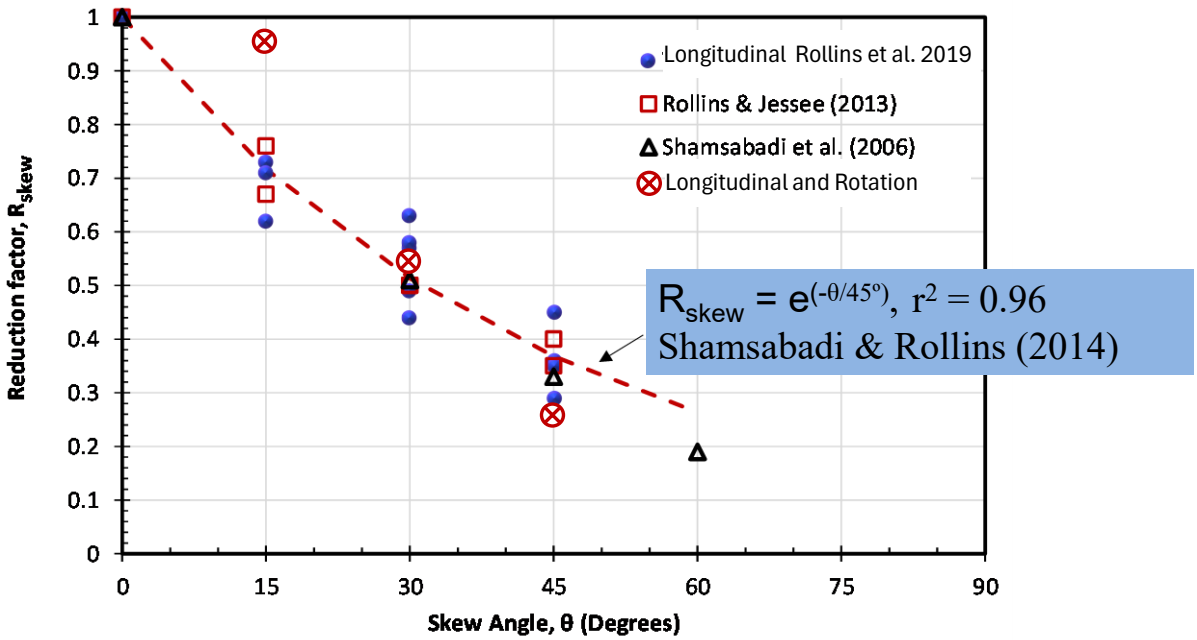

Fig. 5. Plot of passive force reduction factor (R_{skew}) vs. skew angle (Θ) from this study with longitudinal and rotation along with previous longitudinal passive force testing by Rollins and Jessee (2013), Rollins et al. (2019), and data from numerical analyses by Shamsabadi et al. (2006). A best-fit design curve proposed by Shamsabadi & Rollins (2014) is also provided for comparison.